Journal of Applied Polymer Science

Sponge-like chitosan-based nanostructured antibacterial material as a topical hemostat

Ayca Bal-Ozturk,[1,2] Oksan Karal-Yilmaz,[3] Zeynep Puren Akguner,[2] Soner Aksu,[3] Arzu Tas,[3] Hulya Olmez[4]

[1]Faculty of Pharmacy, Department of Analytical Chemistry, Istinye University, Zeytinburnu, Istanbul 34010, Turkey
[2]Institute of Health Sciences, Department of Stem Cell and Tissue Engineering, Istinye University, Zeytinburnu, Istanbul 34010, Turkey
[3]Genetic Engineering and Biotechnology Institute, TUBITAK Marmara Research Center, Gebze, Kocaeli 41470, Turkey
[4]Materials Institute, TUBITAK Marmara Research Center, Gebze, Kocaeli 41470, Turkey
Correspondence to: O. Karal-Yilmaz (E-mail: oksan.yilmaz@tubitak.gov.tr)

ABSTRACT: In this study, chitosan/alginic acid/zinc oxide (CHI/AA/ZnO) nanostructured hydrogel sponges were fabricated by incorporating ZnO nanoparticles (<100 nm) into polymer matrix to develop a new potential biomaterial for hemorrhage control. For this purpose, the crosslinked CHI/AA/ZnO nanostructured sponges were synthesized by freeze-drying technique. Genipin was used as a crosslinker. The prepared chitosan-based sponges were characterized by Fourier transform infrared spectroscopy, X-ray diffraction, and scanning electron microscopy—energy-dispersive spectroscopy analysis. The effects of ZnO content on the physicochemical characteristics of sponge-like nanostructured hydrogels were evaluated by swelling ratio in two different pH values. Physical immobilization of dexamethasone as a model drug in hydrogel matrix resulted sustained release of drug more than 3 days. Antibacterial activity of hydrogel sponges was assessed against *Staphylococcus aureus*. The cytotoxicity and hemostatic efficacy of crosslinked CHI/AA/ZnO sponge like-nanostructured hydrogels was evaluated *in vitro* and *in vivo*, respectively. The results of this study demonstrated that the prepared CHI/AA/ZnO nanostructured sponge had the potential to be an antibacterial topical hemostat. © 2019 Wiley Periodicals, Inc. J. Appl. Polym. Sci. **2019**, *136*, 47522.

KEYWORDS: chitosan hydrogels; genipin; hemorrhage control; ZnO nanoparticles

Received 18 June 2018; accepted 10 December 2018
DOI: 10.1002/app.47522

INTRODUCTION

Uncontrollable hemorrhage remains the pivotal leading cause of deaths worldwide after traumatic or surgical situations on accidents, disasters or battlefields. An urgent effective control of hemorrhage using hemostatic agents could decrease related mortality.[1] Currently, a large number of hemostatic natural and synthetic materials (e.g., chitosan,[2] alginate,[3] cellulose,[3,4] hyaluronic acid,[3] gelatin,[5] collagen,[6] poly(glycolic acid),[6] poly(lactic acid),[7] and poly(vinyl alcohol)[7]) in different forms (e.g., granules, powder, foam, fiber, membrane, hydrogel) have been developed for good biocompatibility, low antigenicity, and rapid hemostatic ability.[5–10] Although an array of hemostatic products is commercially available, disadvantages of these materials concerning biological safety, hemostatic efficacy, and high cost cannot be neglected.[3,11] Therefore, the development of new hemostatic agents is still a challenge. One of the most important limitations of commercially available hemostatic products is bacterial infection on the bleeding area. Since this is very common diagnostic that can delay or impair healing, hemostatic agents with antibacterial behavior are urgently required for improving survival rates.[12]

Among many biomaterials suitable for the hemostatic agent, chitosan (CHI) was selected to prepare sponge-like biomaterial. As known, CHI, natural positively charged linear polysaccharide, has a series of advantages that make it an ideal candidate material for hemorrhage control. The protonated amine groups on CHI backbone could interact with negatively charged residues on red blood cells and platelets and lead thrombus formation.[1] In addition, CHI-based biomaterials have excellent biocompatibility, biodegradability, antibacterial, and wound healing promoting activities.[13] CHI has been used for the fabrication of various polyelectrolyte complex materials with natural and synthetic polyions.[14] In this study, alginic acid (AA) was used to form polyelectrolyte complex with CHI. AA is a rich natural polymer formed by linking of β-D-mannuronic acid (M units) and

α-L-glucuronic acid (G units) monomers.[15] It has high water absorption, ion-exchange ability, biocompatibility, biodegradation potential, and low toxicity. The main problem with these CHI-based scaffolds is the limited stiffness.[13] In order to enhance the mechanical properties, crosslinkers such as glutaraldehyde, epichlorohydrin, carbodiimides, and triphosphate are used to chemically crosslink the polymer network. Genipin, a natural crosslinker, is a widely used crosslinking agent due to the low toxicity property compared to other crosslinkers.[16–19] In addition, genipin crosslinked biomaterials have improved degradative behaviors compared to the glutaraldehyde crosslinked biomaterials. Besides these, genipin itself may also provide an additional therapeutic advantage by virtue of its anti-inflammatory behavior that has been proved by *in vivo* studies.[13]

In recent years, extensive research has been directed toward development the antibacterial polymeric platforms for efficient hemorrhage control.[12,20,21] CHI has inherent antibacterial activity and performs many other advantages for hemostatic activity. However, its antimicrobial activity, coming from polycationic nature, is limited above pH 6.5 due to the starting to lose its cationic nature.[22–24] To enhance the antibacterial behavior, some external antibacterial agents have been incorporated into polymer network. For this purpose, zinc oxide (ZnO) nanoparticles have fascinated researchers because of their good photocatalytic activity, high stability, antibacterial activity, and nontoxicity.[25–28]

In this study, crosslinked CHI/AA/ZnO sponge like-nanostructured hydrogel sponges were synthesized and characterized by Fourier transform infrared spectroscopy (FTIR), X-ray diffraction (XRD), and scanning electron microscopy (SEM) analysis. The swelling behaviors by the immersion in buffer solutions, drug release behaviors, and the antibacterial activities against *Staphylococcus aureus* were also investigated. *In vitro* cytotoxicity of the hydrogel materials was measured by 3-[4,5-dimethylthiazol-2-yl]-2,5-diphenyltetrazolium bromide (MTT) assay. The hemostatic efficacy of crosslinked CHI/AA/ZnO sponge like-nanostructured hydrogels was evaluated *in vivo*.

EXPERIMENTAL

Materials

Chitosan powder (M_v = 109,000 g mol^{-1} and DD = 85%), alginic acid, acetic acid, genipin, and ZnO nanoparticle dispersion (<100 nm particle size, 20 wt % in H_2O), Dulbecco's Modified Eagle's Medium (DMEM), penicillin–streptomycin, MTT, and dimethyl sulfoxide (DMSO) were purchased from Sigma-Aldrich (St. Louis, USA). Fetal bovine serum (FBS) and trypsin-ethylene diamine tetraacetic acid (EDTA, 0.25%) was purchased from GIBCO (Paisley, UK). L-Glutamine was supplied by Biological Industries (Israel). Umbilical cord-derived mesenchymal stem cells (MSCs) were gift from Liv Hospital, Regenerative Medicine, Stem Cell Research and Therapy Center, Istanbul, Turkey.

All other reagents were analytical grade.

Preparation of Genipin Crosslinked Hydrogel Sponges

Genipin crosslinked hydrogel sponges were fabricated by freeze-drying technique.[29,30] Both 2% (w/v) chitosan and alginic acid were prepared in 1% acetic acid and distilled water, respectively. CHI/AA/ZnO solutions were prepared by mixing chitosan and alginic acid solution with different amounts of ZnO nanoparticles. The prepared solutions were stirred for 4 h at room temperature and then 2 mg of genipin was added to each solution. After a quick stirring, polymer solutions were cast on an aluminum dish and then frozen at −20 °C and lyophilized in a freeze-dryer for 3 days. Sponges without genipin (CHI) were prepared in the same manner.

FTIR Spectroscopy Analysis

FTIR spectra were obtained using PerkinElmer Spectrum One Spectrometer equipped with attenuated total reflection (ATR) crystal sampler at room temperature. The lyophilized hydrogel sponges were used directly on an ATR crystal sampler at an absorbance range from 4000 to 400 cm^{-1}.

XRD Analysis

XRD analysis was performed using a Rigaku XRD diffractometer (Cu Kα X-ray source). The lyophilized hydrogel sponges were used directly and XRD runs were carried out over 2θ ranging from 15° to 50° at a scan rate of 1° min^{-1}.

Scanning Electron Microscopy

The morphology of hydrogel sponges was analyzed using a JEOL JSM 6335F type SEM. Hydrogel samples were first cut, then coated with platinum prior to SEM analysis. In addition, energy-dispersive spectroscopy (EDS) was used to investigate the presence of ZnO nanoparticles in the matrix of CHI/AA/ZnO sponge like-nanostructured hydrogels using Oxford Instruments AZtec EDS System attached to the SEM.

Swelling Behavior Study

The swelling behavior of the hydrogel sponges under two different conditions was investigated by immersing the lyophilized samples (~10 mg) in buffer solutions (pH 7.4 and 2.0) at 37 °C.[30] After 48 h, the swollen samples were removed from the buffer solutions and blotted with a piece of filter paper to remove excess water on the hydrogel surface. The weight of the swollen sponge was measured and the swelling ratio (S) was then calculated with the following equation:

$$S = (W_t - W_0)/W_0 \quad (1)$$

where S is the swelling ratio of the sponge, and W_0 and W_t are the weight of the dried sponge and the swollen sponge, respectively.

Drug Loading and *In Vitro* Drug Release Studies

Dexamethasone (DEX) was selected as a model drug. First, 3 mg of DEX was dissolved in 1 mL of ethanol[31] before mixing with 20 mL of polymer solutions at the rates given in Table I. Then, DEX-loaded hydrogels were prepared according to the same process described in the Preparation of Genipin Crosslinked Hydrogel Sponges section.

For *in vitro* drug release experiments, DEX-loaded hydrogel samples were immersed in phosphate-buffered saline (PBS; pH 7.4). The experiments were carried out at 37 °C with gentle shaking (100 rpm). At regular time intervals, 2 mL aliquots of the release medium were replaced with fresh PBS and the concentration

Table I. The Sample Codes and Feed Compositions of Hydrogel Sponges

Sample code	ZnO suspension (μL)	Genipin (mg)	Chitosan solution (mL)	Alginic acid (mL)
CHI	—	—	20	—
CHI/AA	—	2	10	10
CHI/AA/ZnO-1	12	2	10	10
CHI/AA/ZnO-2	24	2	10	10
CHI/AA/ZnO-3	48	2	10	10

DEX in that aliquot was measured by using a ultraviolet (UV) spectrophotometer at 242 nm.[32]

Antibacterial Study

The bacterial culture of *S. aureus* ATCC 25923 was grown on nutrient agar slants and stored at 4 °C. A loopful of bacteria from the agar slant was transferred into 15 mL tryptic soy broth in a sterile centrifuge tube and incubated at 35 °C for 24 h. The bacterial culture for antibacterial activity testing was diluted to a concentration of 10^7 cfu mL^{-1} to obtain the test suspension. Antibacterial activity of the sponge-like chitosan samples was assessed using the disc diffusion and the plate count technique. Antibacterial activity tests were performed using chitosan samples, which were cut into a disc form of 6 mm in diameter using a sterile circular cutting die.

For the disc diffusion method, the chitosan discs of each of the sample were placed on Baird-Parker agar plates, which were initially inoculated with 0.1 mL of *S. aureus* suspension in the range of 10^6 cfu mL^{-1}. The plates were incubated at 37 °C for 24 h. The diameter of the inhibition zone surrounding the chitosan discs was measured. For the quantitative assessment of the antibacterial activity, the chitosan discs were placed into 15 mL sterile tubes. Then, 200 μL of the *S. aureus* suspension was transferred into each tube. After 2–3 min, 800 μL of PBS (pH 7.4) was added to each tube and incubated in a shaking incubator at 37°C for 24 h. Serial dilutions from each sample were spread inoculated on Baird-Parker agar plates and incubated at 35°C for 24 h before the colonies were counted. The experiments were performed in triplicate. Data points are expressed as means ± standard deviations. Differences between the means were analyzed using Student's *t* test, taking $p < 0.05$ as statistically significant.

In Vitro Cytotoxic Evaluation

The *in vitro* indirect cytotoxicity of hydrogel samples was determined according to the literature.[1] Umbilical cord-derived MSCs were used to determine cytotoxic effect of extracts of hydrogel samples. MSCs were cultured at 37 °C in a humid atmosphere of 5% CO_2 in DMEM, supplemented with 10% FBS, 1% penicillin/streptomycin, and 1% L-glutamine. The culture medium was changed every 2 days. When the MSCs reached 80% confluence, they were digested with 0.25% trypsin-0.02% EDTA and then suspended in DMEM. Cells were collected by centrifuging at 1500 rpm for 5 min.

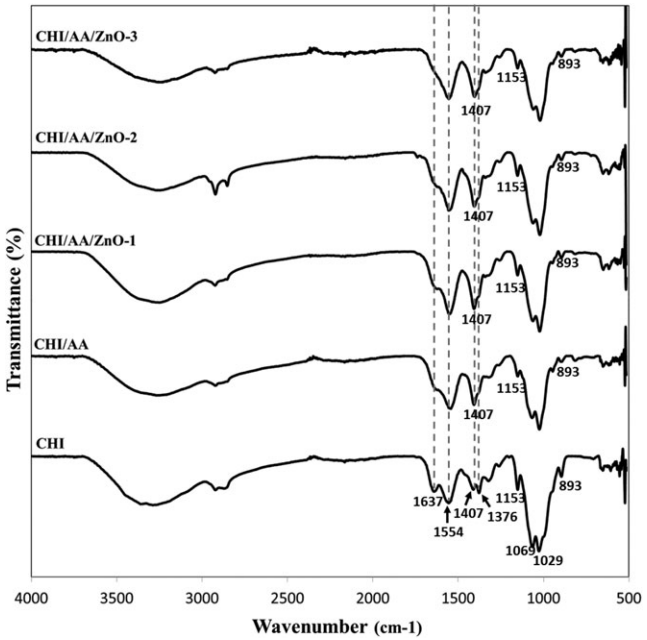

Figure 2. The FTIR spectra of CHI, CHI/AA, CHI/AA/ZnO-2, and CHI/AA/ZnO-3 hydrogel sponges.

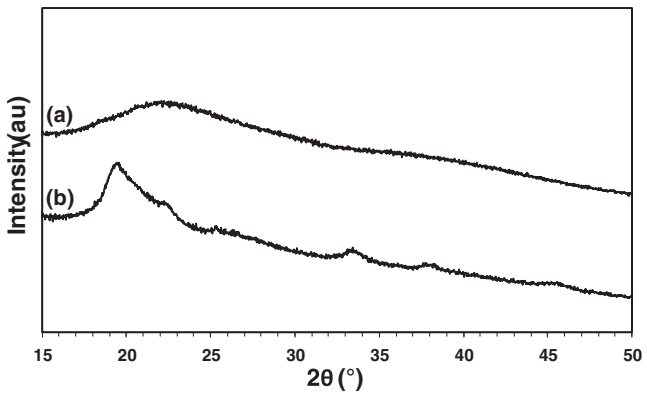

Figure 3. The XRD spectra of (a) CHI/AA and (b) CHI/AA/ZnO-3 hydrogel sponges.

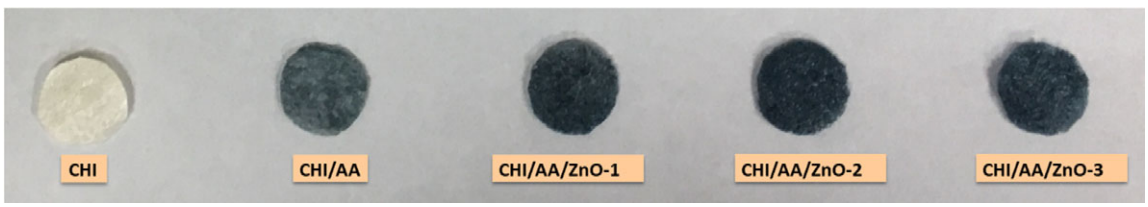

Figure 1. Images of freeze-dried hydrogel sponges. Different shades of the blue color are an indication of genipin-crosslinking reaction. [Color figure can be viewed at wileyonlinelibrary.com]

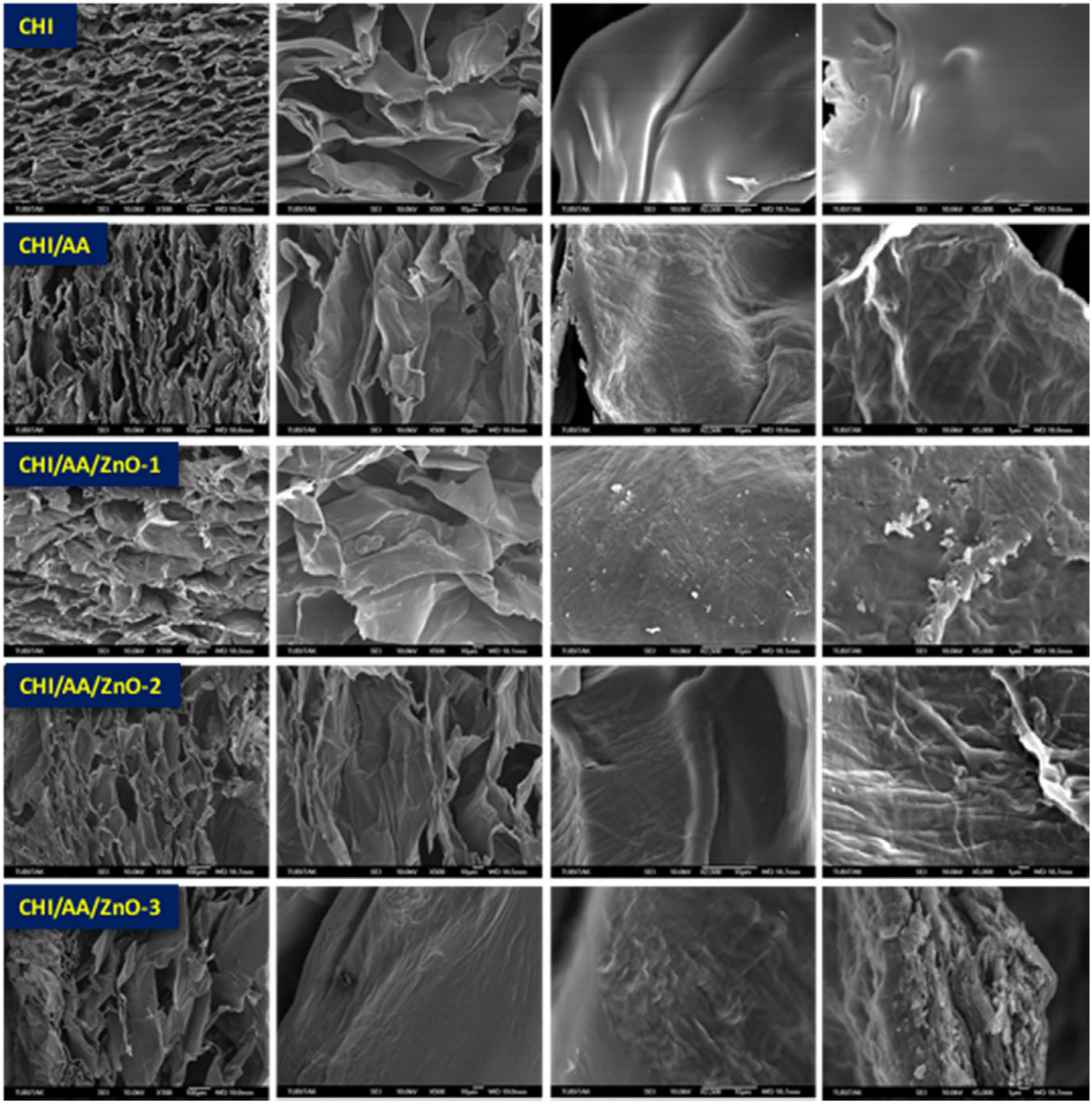

Figure 4. SEM images of CHI, CHI/AA, and CHI/AA/ZnO hydrogel sponges. [Color figure can be viewed at wileyonlinelibrary.com]

Both sides of the samples were sterilized under UV light for 30 min. To extract potential cytotoxic residues, the sterile samples were incubated with MSCs culture medium at 37 °C for 24 h with an extraction ratio of 1 cm^2 mL^{-1}.[33] After the incubation period, the hydrogel samples were removed and the incubated media with samples were diluted twofold in fresh MSCs culture medium. *In vitro* cytotoxic activity of hydrogel samples was assessed using MTT assay. MSCs from passages number 5 were seeded in 48-well plates at a density of 1×10^4 cells/well in 300 μL MSCs culture medium and incubated at 37 °C in 5% CO_2 atmosphere for 24 h. The culture medium was then replaced with the prepared medium as mentioned above and was incubated for another 24 h. After the incubation period, the medium was removed and 300 μL DMEM and 50 μL MTT in sterile PBS (20 μg mL^{-1}) was added to each well. After another 2 h incubation, the medium was replaced with 300 mL DMSO and read at 570 nm using a microplate reader after 20 min incubation.

In Vivo Evaluation

The hemostatic effect test was performed using six New Zealand rabbits, weighing <2 kg. Rabbit ear peripheral capillary hemorrhage model was created by forming an "L" incision in the ear

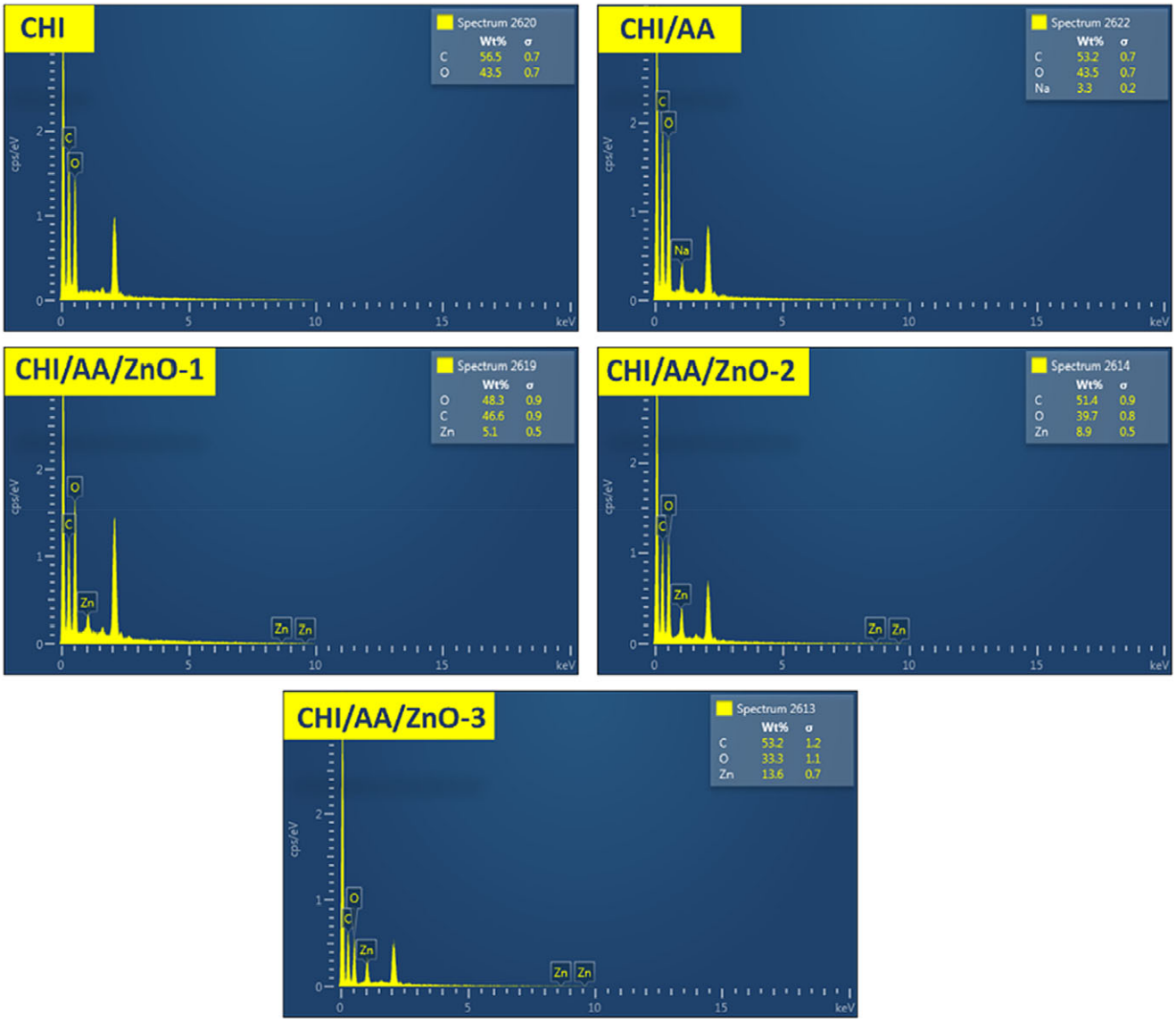

Figure 5. EDS images of CHI, CHI/AA, and CHI/AA/ZnO hydrogel sponges. [Color figure can be viewed at wileyonlinelibrary.com]

tip region of the middle ear axis.[34] *In vivo* operations were performed under general anesthesia (ketamine 35 mg kg^{-1} + xylazine 5 mg kg^{-1}).[35] The test was carried out by applying CHI, CHI/AA, CHI/AA/ZnO-1, and control samples (Oxidized Regenerated Cellulose Absorbable Hemostat) to be tested on the wound after the first bloodshed. When the samples were applied to the bleeding zone, a weight of about 114.96 g was applied to create a pressure of 3 N force. One ear of the test animals was used for the main product and the other ear was used for the control product. After the application of the sample bleeding was observed every 30 s. The duration of the bleeding and the amount of bleeding was tried to be determined by weighing the tested sample after the bleeding.

RESULTS AND DISCUSSION

New sponge-like chitosan-based nanostructured antibacterial materials were successfully synthesized via freeze-drying technique and characterized by FTIR, XRD, and SEM–EDS analysis for the potential use in biomedical applications as the antibacterial hemostatic agent. The effects of amount of ZnO nanoparticles on the physicochemical characteristics of sponge-like nanostructured hydrogels were evaluated by swelling ratio and antibacterial activity against gram positive and negative bacteria, *in vitro* cytotoxicity and *in vivo* hemostatic efficacy of the hydrogels was investigated.

The successful crosslinking of polymer network with genipin was confirmed by significant color change in the hydrogel sponges from white to blue color (Figure 1). In addition, there is a color differences between genipin crosslinked hydrogels. The color of ZnO nanostructured hydrogels is deeper blue than CHI/AA hydrogel. According to the literature, altering the pH within the small range of 4.00–5.50 dramatically affects the reaction, leading to hydrogels differing both in appearance and in properties. This is because the degree of chitosan protonation depends on pH and the protonated chitosan reacts with genipin.[19]

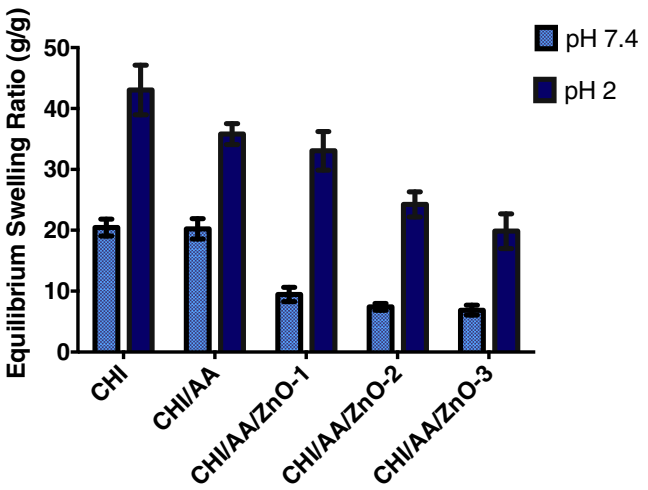

Figure 6. Swelling behaviour of CHI, CHI/AA, CHI/AA/ZnO-1, CHI/AA/ZnO-2, and CHI/AA/ZnO-3 in pH 7.4 and pH 2.0. [Color figure can be viewed at wileyonlinelibrary.com]

Figure 2 displays FTIR–ATR spectra of CHI, CHI/AA, and CHI/AA/ZnO sponges. The spectrum of chitosan-based sponge without genipin (CHI) shows absorption peaks at 1637, 1554, and 1069 cm^{-1} assigned to the C=O stretching (Amide I band), N-H deformation (Amide II band) and C-O stretching vibration, respectively. In addition, the representative bands of CHI around 893 and 1153 cm^{-1} were due to the asymmetric stretching vibrations of C-O-C of the saccharide structure.[1,36–39] As observed from the FTIR spectra of the CHI/AA and CHI/AA/ZnO sponges, the adsorption band intensity at 1637 cm^{-1} decreased while the sharp adsorption band at 1407 cm^{-1} revealed. These findings are attributed to the formation of secondary amide linkages due to the reaction of carboxymethyl units of genipin and the amino units of chitosan.[36,38,40] According to the FTIR spectra of hydrogels incorporating ZnO nanoparticles, the broadening peaks around 3450 cm^{-1} attributed to the intermolecular hydrogen bonding between the ZnO nanoparticles and chitosan.[25] In addition, the absorption peak observed at the range of 500–580 cm^{-1} are ascribed to the vibration of O-Zn-O groups, which confirming the presence of ZnO nanoparticles in the polymer matrix due to the hydrogen bonds between ZnO and CHI.[41,42]

XRD patterns of CHI/AA and CHI/AA/ZnO-3 hydrogel sponges are shown in Figure 3. CHI/AA hydrogel sponges have no sharp diffraction peaks except a broadband in the range of $2\theta = 18°–25°$ which imply the amorphous nature of the hydrogel structure. In addition, CHI/AA/ZnO-3 nanostructured hydrogel sponges showed three additional peaks at 2θ values of 33°, 38°, and 45° which were related to the ZnO crystallite.[41] These characteristic peaks in the XRD pattern of CHI/AA/ZnO-3 nanostructured hydrogel sponge indicated that ZnO particles were successfully loaded into CHI/AA sponge, supporting the SEM–EDS results. In addition, characteristic peaks of ZnO nanoparticles are not seen in the spectra of CHI/AA/ZnO-1 and CHI/AA/ZnO-2 hydrogel (data not shown) the reason of which may be the slight presence of ZnO in hydrogel structure.[43]

SEM images of CHI/AA and CHI/AA/ZnO nanostructured hydrogel sponges are presented in Figure 4. The hydrogel sponges include microporous network with interconnected pores in that are surrounded by polymer walls. SEM images show that adding ZnO nanoparticles causes a reduction in the porosity of hydrogel sponges, which is due to the formation of intermolecular hydrogen bonding between polymer network and ZnO nanoparticles.[44] This interaction causes the polymer chains of chitosan to be packed together leading to a reduction in porosity. The presence of ZnO nanoparticles in the nanostructured hydrogel networks was evident from the SEM–EDS experiments (Figure 5).

Swelling capacity of the hemostatic agents has an important role for prevention of loss of body fluid.[45] In this work, swelling behavior of the hydrogel sponges upon exposure to two different swelling media (pH 2.0 and pH 7.4) and influence of different amounts of ZnO nanoparticles on swelling behavior was studied (Figure 6). All sponges were swelled higher in the acidic conditions than in neutral conditions. It is expected that $-NH_2$ groups on the hydrogel chain get protonated under acidic conditions.[46,47] The electrostatic repulsion of this protonated amine groups on chitosan backbone could cause to an expansion of the hydrogel network and thus a higher swelling.[48] The swelling ratio of the CHI/AA and CHI/AA/ZnO nanostructured hydrogel sponges seems to slightly decrease as the ZnO nanoparticles were incorporated in the hydrogel sponges to cause a more crosslink bond. This is related to the connection of ZnO nanoparticles and electrons of oxygen and hydrogen atoms of hydroxyl groups and amines existing in CHI and AA chains[44] to

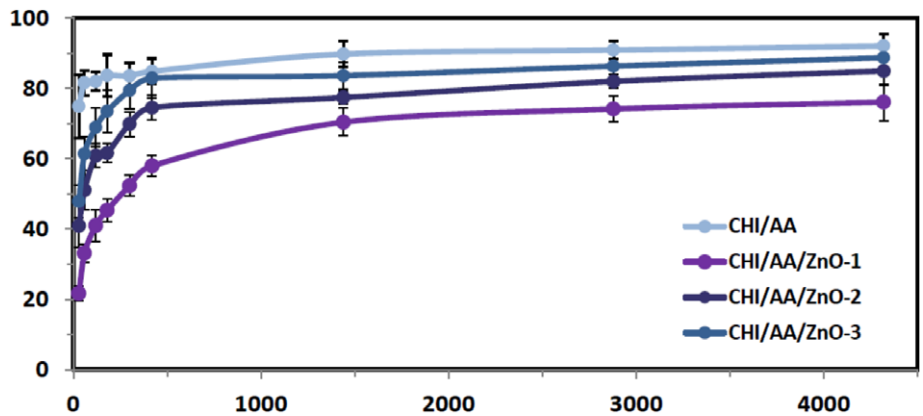

Figure 7. DEX release profiles of CHI/AA and CHI/AA/ZnO hydrogel sponges at pH 7.4 at 37°. [Color figure can be viewed at wileyonlinelibrary.com]

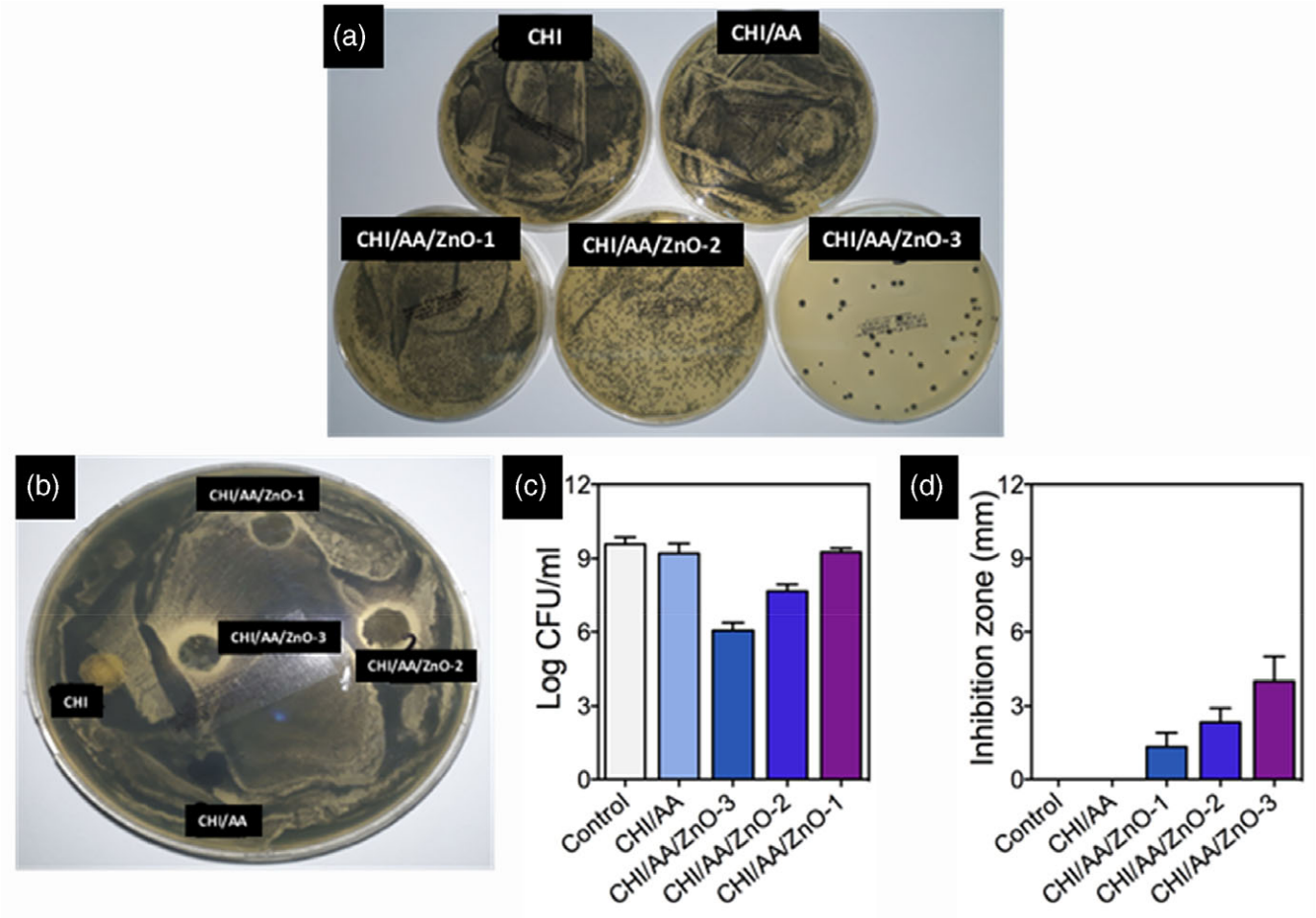

Figure 8. (a) Baird-Parker agar Petri plate images of *S. aureus* inoculated samples after incubation at 37 °C for 24 h. (b) Inhibition zones of hydrogel sponges. (c) *S.aureus* counts of CHI, CH/AA, CHI/AA/ZnO-1, CHI/AA/ZnO-2, and CHI/AA/ZnO-3 samples after 24 h of incubation at 37 °C. (d) Inhibition zones in mm for chitosan samples on *S. aureus* plates. [Color figure can be viewed at wileyonlinelibrary.com]

closely wrap the polymer chains.[49] As a result, the hydrogel network contains additional cavities in which water is trapped and a decrease in swelling behavior is observed.

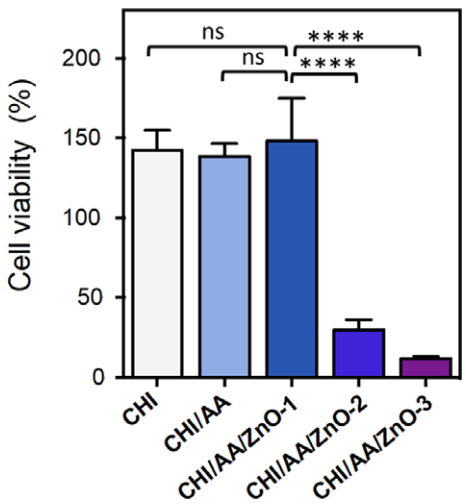

Figure 9. Cytotoxicity of CH/AA, CHI/AA/ZnO-1, CHI/AA/ZnO-2, and CHI/AA/ZnO-3 samples against MSCs after 24 h. [Color figure can be viewed at wileyonlinelibrary.com]

In vitro drug release profiles of the hydrogel sponges are presented in Figure 7. DEX release was found to be 91.9, 76.1, 85.0, and 88.7% from CHI/AA, CHI/AA-ZnO-1, CHI/AA-ZnO-2, and CHI/AA-ZnO-3, respectively, in 4300 min (approximately 3 days). DEX release (%) from the hydrogels was higher in the CHI/AA than CHI/AA/ZnO nanostructured hydrogels, which was mainly due to higher swelling of hydrogels in pH 7.4, as discussed above. As it is obvious, there is a significant decrease in the drug release from the CHI/AA-ZnO-1 hydrogel sponges. Because the releasing time of drug from nanostructured hydrogel sponges is prolonged due to a longer path required for DEX to

Table II. Mean and Standard Deviation Value of Test and Control Groups for Hemostatic Time and Total Blood Loss

Samples	Total blood loss (mg)	Hemostatic time (s)
CHI	610 ± 339.41	137 ± 24.75
CHI/AA	365 ± 91.92	85 ± 7.07
CHI/AA/ZnO-1	263 ± 168.62	93 ± 10.41
Positive control	70 ± 28.28	60 ± 0
Negative control	973 ± 50.33	—

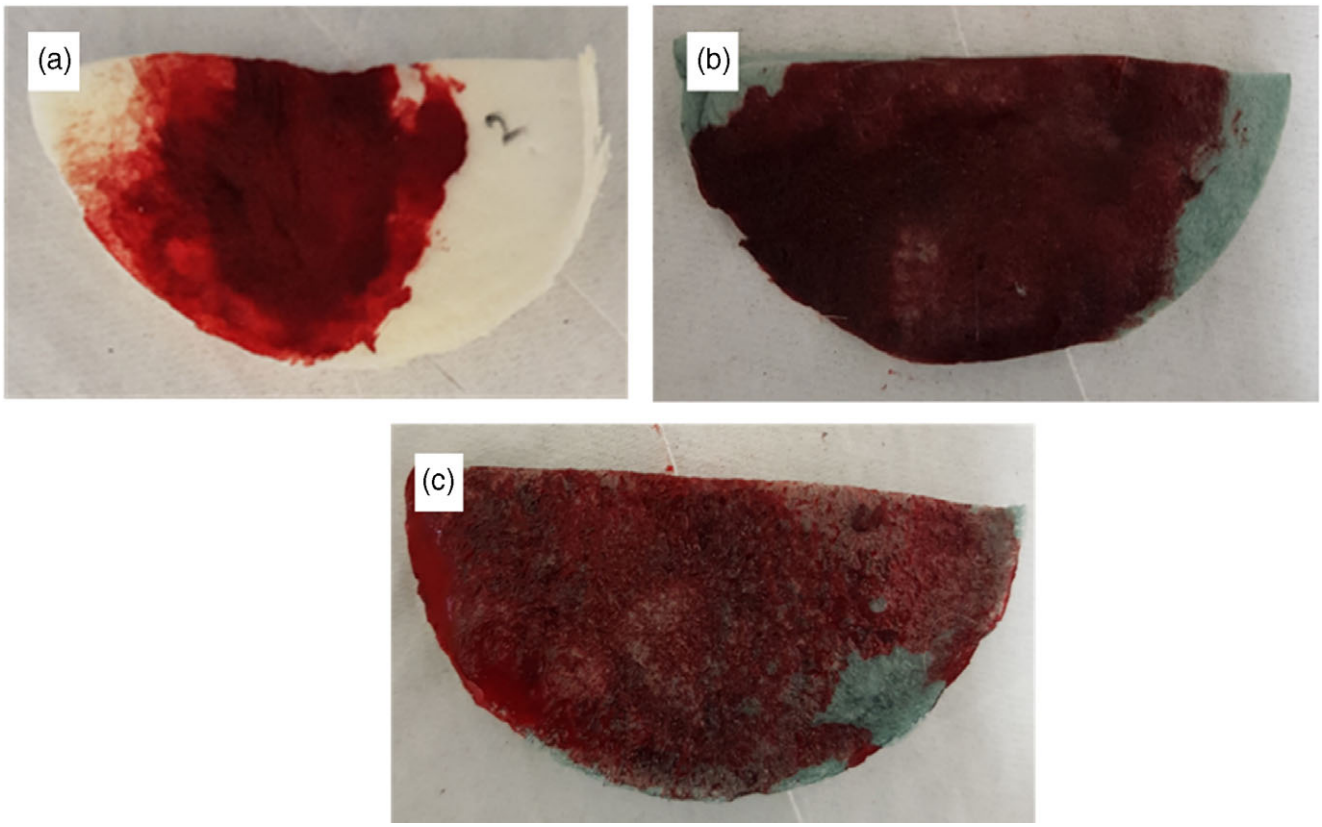

Figure 10. Peripheral capillary bleeding in the ear tip region of the middle ear stopped by hydrogel sponges: (a) CHI, (b) CHI/AA, and (c) CHI/AA/ZnO-1. [Color figure can be viewed at wileyonlinelibrary.com]

move from the CHI/AA-ZnO-1 hydrogel sponges to the release medium compared with the neat hydrogel sponges.[41,50] On the other hand, DEX release rate exhibited a tendency to increase while ZnO amount increased in the hydrogel network. This is because ZnO aggregation exists into the hydrogel network when ZnO amount is above a certain concentration in the medium.[50,51]

Antibacterial activity of chitosan-based hydrogel sponges was assessed against *S. aureus* using the disc diffusion and the plate count techniques. As shown in Figure 8(a,b), the CHI/AA/ZnO-3 samples showed the highest inhibition zone, and the lowest final *S. aureus* counts after 24 h of incubation at 37 °C. Compared to the CHI sample, significant inhibition of the *S. aureus* growth was observed for all of the ZnO incorporated hydrogel sponges. Having the highest ZnO content, the CHI/AA/ZnO-3 samples showed significantly higher ($p < 0.05$) bacteriostatic effect compared to the other samples [Figure 7(c,d)].

Biocompatibility is a primary requirement for wound dressing applications.[38] An ideal topically used hemostatic dressing should not release toxic products or produce adverse reactions.[52] In this context, the level of cytotoxicity of CH/AA, CHI/AA/ZnO-1, CHI/AA/ZnO-2, and CHI/AA/ZnO-3 hydrogel sponges toward cell viability were performed by means of indirect MTT assay according to the literature. MSCs were incubated in the extracted medium from hydrogel samples. Cell viability results are presented in Figure 9. CHI, CHI/AA, and CHI/AA/ZnO-1 hydrogel samples show no toxicity within 24 h and no statistical differences were observed between these products. In addition, the increase of ZnO nanoparticle concentration into the hydrogel sponges, CHI/AA/ZnO-2 and CHI/AA/ZnO-3, led to significant decrease in cell viability (<50%). This means that only CHI/AA/ZnO-1 product, containing the least amount of ZnO nanoparticles, does not have any negative release into the medium. Consequently, the obtained results indicated that CHI/AA/ZnO-1 hydrogel sponge had no toxicity making it an ideal material for wound dressing.

In this study, CHI/AA/ZnO nanostructured hydrogel sponges were fabricated as a potential antibacterial biomaterial for hemorrhage control. Their effectiveness on hemostasis was evaluated by ear peripheral capillary hemorrhage model *in vivo*. The hemostatic time was measured and total blood loss in animals was weighted as shown in Table II. The total blood loss in the CHI, CHI/AA, and CHI/AA/ZnO-1 groups (Figure 10) were found to be 610 ± 339.41, 365 ± 91.92, and 263 ± 168.62 mg, respectively. In addition, hemostatic time in CHI/AA group (93 ± 10.41 s) was shorter than in the CHI (137 ± 24.75 s) and CHI/AA/ZnO-1 (93 ± 10.41 s) groups. According to these results, CHI/AA hydrogel seems to have the lowest time and has the closest bleeding time to the positive control group. At this point, it was seen that the CHI hydrogel has the longest average bleeding time. On the other hand, the difference between CHI/AA/ZnO-1 hydrogel and positive test groups seems to be statistically significant in terms of bleeding time. When the groups were evaluated in terms of weight difference, it was seen that the CHI hydrogel had the highest amount of bleeding in accordance with the findings of the bleeding

time. CHI/AA is more flexible and thin than CHI hydrogel. This form was advantageous in terms of product penetration into the wound. It was rapidly softened and sticks to the wound when it came into contact with blood. So, the tissue penetration into the bleeding point was more successful. This result showed that blood sucking property of the CHI/AA hydrogel was also more successful. On the other hand, CHI/AA/ZnO-1 hydrogel also show a more rigid structure than CHI. When it came into contact with blood, it hardly softened like CHI products, which was a problem in terms of tissue penetration in wound region. As a result, the clinical application of these results in the future studies may provide a standard information after a detail optimization experiments to adjust the best ZnO ratio in polymer matrix.

CONCLUSIONS

In this study, a new sponge-like chitosan-based nanostructured antibacterial material was synthesized and characterized for the potential use in biomedical applications as the hemostatic agent. According to the SEM images, all hydrogel samples include microporous network with interconnected pores in that are surrounded by polymer walls. The presence of ZnO nanoparticles in the nanostructured hydrogel networks was evident from the XRD and SEM–EDS results. In antibacterial experiments, ZnO incorporated hydrogel sponges had good bacteriostatic effect on *S. aureus* antibacterial property increased with the increase of ZnO amount in polymer network. *In vitro* cytotoxicity evaluation studies confirmed the biocompatibility of CHI/AA/ZnO-1 nanostructured hydrogel sponges. In addition, by performing *in vivo* bleeding models, it was demonstrated that CHI/AA/ZnO-1 nanostructured hydrogel sponges can be potential candidate as a topical hemostat for controlling wound infection.

ACKNOWLEDGMENTS

Financial support for this research was provided by the TUBITAK (The Scientific and Technological Research Council of Turkiye) project number 5143401.

REFERENCES

1. Chen, Q.; Liu, Y.; Wang, T.; Wu, J.; Zhai, X.; Li, Y.; Zhao, X. *J. Mater. Chem. B.* **2017**, *5*(20), 3686.
2. Gu, B. K.; Park, S. J.; Kim, M. S.; Kang, C. M.; Kim, J. I.; Kim, C. H. *Carbohydr. Polym.* **2013**, *97*(1), 65.
3. Yang, X.; Liu, W.; Li, N.; Wang, M.; Liang, B.; Ullah, I.; Shi, C. *Biomater. Sci.* **2017**, *5*(12), 2357.
4. Li, H.; Cheng, W.; Liu, K.; Chen, L.; Huang, Y.; Wang, X.; Li, C. *Carbohydr. Polym.* **2017**, *165*, 30.
5. Gaharwar, A. K.; Avery, R. K.; Assmann, A.; Paul, A.; McKinley, G. H.; Khademhosseini, A.; Olsen, B. D. *ACS Nano*. **2014**, *8*(10), 9833.
6. Yan, T.; Cheng, F.; Wei, X.; Huang, Y.; He, J. *Carbohydr. Polym.* **2017**, *170*, 271.
7. Zhang, Y.; Song, D.; Huang, H.; Liang, Z.; Liu, H.; Huang, Y.; Ye, G. *Sci. Rep.* **2017**, *7*(1), 15250.
8. Sun, X.; Tang, Z.; Pan, M.; Wang, Z.; Yang, H.; Liu, H. *Carbohydr. Polym.* **2017**, *177*, 135.
9. Lan, G.; Lu, B.; Wang, T.; Wang, L.; Chen, J.; Yu, K.; Wu, D. *Colloids Surf. B.* **2015**, *136*, 1026.
10. Zhao, X.; Wu, H.; Guo, B.; Dong, R.; Qiu, Y.; Ma, P. X. *Biomaterials*. **2017**, *122*, 34.
11. Zhang, H.; Lv, X.; Zhang, X.; Wang, H.; Deng, H.; Li, Y.; Li, X. *RSC Adv.* **2015**, *5*(62), 50523.
12. Landsman, T. L.; Touchet, T.; Hasan, S. M.; Smith, C.; Russell, B.; Rivera, J.; Cosgriff-Hernandez, E. *Acta Biomater.* **2017**, *47*, 91.
13. Gao, L.; Gan, H.; Meng, Z.; Gu, R.; Wu, Z.; Zhang, L.; Dou, G. *Colloids Surf. B.* **2014**, *117*, 398.
14. Giri, T. K.; Thakur, A.; Alexander, A.; Badwaik, H.; Tripathi, D. K. *Acta Pharm. Sin. B.* **2012**, *2*(5), 439.
15. Li, X.; Kong, X.; Zhang, Z.; Nan, K.; Li, L.; Wang, X.; Chen, H. *Int. J. Biol. Macromol.* **2012**, *50*(5), 1299.
16. Bi, L.; Cao, Z.; Hu, Y.; Song, Y.; Yu, L.; Yang, B.; Han, Y. *J. Mater. Sci. Mater. Med.* **2011**, *22*(1), 51.
17. Nath, S. D.; Abueva, C.; Kim, B.; Lee, B. T. *Carbohydr. Polym.* **2015**, *115*, 160.
18. Cheng, N. C.; Estes, B. T.; Young, T. H.; Guilak, F. *Tissue Eng. Part A*. **2012**, *19*(3–4), 484.
19. Delmar, K.; Bianco-Peled, H. *Carbohydr. Polym.* **2015**, *127*, 28.
20. Dai, C.; Yuan, Y.; Liu, C.; Wei, J.; Hong, H.; Li, X.; Pan, X. *Biomaterials*. **2009**, *30*(29), 5364.
21. Hou, Y.; Xia, Y.; Pan, Y.; Tang, S.; Sun, X.; Xie, Y.; Wei, J. *Mater. Sci. Eng. C.* **2017**, *76*, 340.
22. Lim, S. H.; Hudson, S. M. *Carbohydr. Res.* **2004**, *339*(2), 313.
23. Yang, T. C.; Chou, C. C.; Li, C. F. *Int. J. Food Microbiol.* **2005**, *97*(3), 237.
24. Goy, R. C.; Britto, D. D.; Assis, O. B. *Polímeros*. **2009**, *19*(3), 241.
25. Sudheesh Kumar, P. T.; Lakshmanan, V. K.; Anilkumar, T. V.; Ramya, C.; Reshmi, P.; Unnikrishnan, A. G.; Jayakumar, R. *ACS Appl. Mater. Interfaces*. **2012**, *4*(5), 2618.
26. Bui, V. K. H.; Park, D.; Lee, Y. C. *Polymers*. **2017**, *9*(1), 21.
27. Cahú, T. B.; Silva, R. A.; Silva, R. P.; Silva, M. M.; Arruda, I. R.; Silva, J. F.; Bezerra, R. S. *Appl. Biochem. Biotechnol.* **2017**, *183*(3), 765.
28. Suwannamek, N.; Ruangpaisarn, N.; Prahsan, C. *Mater. Sci. Forum*. **2013**, *761*, 103.
29. Li, Y.; Samad, Y. A.; Polychronopoulou, K.; Alhassan, S. M.; Liao, K. *Sci. Rep.* **2014**, *4*, 4652.
30. Echazú, M. I. A.; Olivetti, C. E.; Anesini, C.; Perez, C. J.; Alvarez, G. S.; Desimone, M. F. *Mater. Sci. Eng. C.* **2017**, *81*, 588.
31. Dong, K.; Dong, Y.; You, C.; Xu, W.; Huang, X.; Yan, Y.; Xing, J. *Drug Deliv.* **2016**, *23*(1), 174.
32. Sahle, F. F.; Gerecke, C.; Kleuser, B.; Bodmeier, R. *Int. J. Pharm.* **2017**, *516*(1–2), 21.
33. Alavarse, A. C.; de Oliveira Silva, F. W.; Colque, J. T.; da Silva, V. M.; Prieto, T.; Venancio, E. C.; Bonvent, J. J. *Mater. Sci. Eng. C.* **2017**, *77*, 271.

34. Wu, Y.; He, J.; Cheng, W.; Gu, H.; Guo, Z.; Gao, S.; Huang, Y. *Carbohydr. Polym.* **2012**, *88*(3), 1023.
35. Lipman, N. S.; Marini, R. P.; Erdman, S. E. *Lab. Anim. Sci.* **1990**, *40*(4), 395.
36. Mi, F. L.; Sung, H. W.; Shyu, S. S. *Carbohydr. Polym.* **2002**, *48*(1), 61.
37. Dimida, S.; Barca, A.; Cancelli, N.; De Benedictis, V.; Raucci, M. G.; Demitri, C. *Int. J. Polym. Sci.* **2017**, *2017*, 1.
38. Chiono, V.; Pulieri, E.; Vozzi, G.; Ciardelli, G.; Ahluwalia, A.; Giusti, P. *J. Mater. Sci. Mater. Med.* **2008**, *19*(2), 889.
39. Zhao, X.; Li, Z.; Pan, H.; Liu, W.; Lv, M.; Leung, F.; Lu, W. W. *Acta Biomater.* **2013**, *9*(5), 6694.
40. Shao, W.; Wu, J.; Wang, S.; Huang, M.; Liu, X.; Zhang, R. *Carbohydr. Polym.* **2017**, *157*, 1963.
41. Zare-Akbari, Z.; Farhadnejad, H.; Furughi-Nia, B.; Abedin, S.; Yadollahi, M.; Khorsand-Ghayeni, M. *Int. J. Biol. Macromol.* **2016**, *93*, 1317.
42. Youssef, A. M.; Abou-Yousef, H.; El-Sayed, S. M.; Kamel, S. *Int. J. Biol. Macromol.* **2015**, *76*, 25.
43. Khorasani, M. T.; Joorabloo, A.; Moghaddam, A.; Shamsi, H.; MansooriMoghadam, Z. *Int. J. Biol. Macromol.* **2018**, *114*, 1203.
44. Baghaie, S.; Khorasani, M. T.; Zarrabi, A.; Moshtaghian, J. *J. Biomater. Sci. Polym. Ed.* **2017**, *28*(18), 2220.
45. Chen, Y.; Zhang, Y.; Wang, F.; Meng, W.; Yang, X.; Li, P.; Zheng, Y. *Mater. Sci. Eng. C.* **2016**, *63*, 18.
46. Hiremath, J. N.; Vishalakshi, B. *Der Pharma Chem.* **2012**, *4*(3), 946.
47. Liu, Y.; Lu, J.; Li, M.; He, C. *Polymer*. **2016**, *40*(2), 1.
48. Liu, Y.; Kim, H. I. *Carbohydr. Polym.* **2012**, *89*(1), 111.
49. Vasile, B. S.; Oprea, O.; Voicu, G.; Ficai, A.; Andronescu, E.; Teodorescu, A.; Holban, A. *Int. J. Pharm.* **2014**, *463*(2), 161.
50. Yadollahi, M.; Farhoudian, S.; Barkhordari, S.; Gholamali, I.; Farhadnejad, H.; Motasadizadeh, H. *Int. J. Biol. Macromol.* **2016**, *82*, 273.
51. Omar, F. M.; Aziz, H. A.; Stoll, S. *Int. J. Chem. Environ. Eng.* **2014**, *468*, 195.
52. Raafat, A. I.; El-Sawy, N. M.; Badawy, N. A.; Mousa, E. A.; Mohamed, A. M. *Int. J. Biol. Macromol.* **2018**, *118*, 1892.